PHYSICAL REVIEW B **82**, 041105(R) (2010)

Comparative study of $FeCr_2S_4$ and $FeSc_2S_4$: Spinels with orbitally active *A* site

S. Sarkar,[1] T. Maitra,[2] Roser Valentí,[3] and T. Saha-Dasgupta[1]
[1]*S. N. Bose National Centre for Basic Sciences, Kolkata, India*
[2]*Department of Physics, Indian Institute of Technology, Roorkee, India*
[3]*Institut für Theoretische Physik, Goethe Universität, Frankfurt, Germany*
(Received 13 June 2010; published 26 July 2010)

Using first-principles density-functional calculations, we perform a comparative study of two Fe-based spinel compounds, $FeCr_2S_4$ and $FeSc_2S_4$. Though both systems contain an orbitally active *A* site with an Fe^{2+} ion, their properties are rather dissimilar. Our study unravels the microscopic origin of their behavior driven by the differences in hybridization of Fe *d* states with Cr/Sc *d* states and S *p* states in the two cases. This leads to important differences in the nature of the magnetic exchanges as well as the nearest-versus next-nearest-neighbor exchange parameter ratios, resulting into significant frustration effects in $FeSc_2S_4$ which are absent in $FeCr_2S_4$.

DOI: 10.1103/PhysRevB.82.041105 PACS number(s): 71.20.Be, 71.15.Mb, 71.70.Ej

Spinel compounds have attracted a lot of attention in the last years due to the intricate interplay of spin, charge, and orbital degrees of freedom together with intrinsic frustration effects driven by their peculiar geometry. A large amount of work has been done on normal spinels of general formula AB_2X_4 with tetrahedral AX_4 and octahedral BX_6 units, and with orbitally active *B* sites such as ZnV_2O_4,[1–4] MnV_2O_4,[5–7] CdV_2O_4,[1] $CuIr_2S_4$,[8] or $MgTi_2O_4$.[9] Examples of compounds with orbitally active *A* sites also exist, as is the case of $FeCr_2S_4$ (FCS) and $FeSc_2S_4$ (FSS). The Fe^{2+} ion in these cases is in a $3d^6$ configuration with a local $S=2$ moment and a twofold orbital degeneracy associated with one hole in a doubly degenerate *e* state of the tetrahedrally crystal split *d* levels. In FCS, the *B* cation is magnetic (Cr^{3+} has a spin $S=3/2$) while for FSS, the *B* cation is nonmagnetic (Sc^{3+} has a filled shell [Ar] configuration). FCS orders magnetically in a ferrimagnetic spin arrangement between Fe and Cr moments with a transition temperature[10] of 167 K while FSS does not order magnetically down to a measured temperature of 50 mK.[11] FCS shows long-range orbital order in polycrystalline samples while a glassy freezing has been observed in single crystals. FSS, in contrast, has been reported as an orbital liquid.[12]

Considering the measured Curie-Weiss temperature (Θ_{CW}) of −200 K [FCS (Ref. 12)] and −45 K [FSS (Ref. 12)], the frustration parameter defined as $f=\frac{-\Theta_{CW}}{T_N}$, T_N being the magnetic transition temperature, is 1.2 for FCS and larger than 1000 for FSS. To best of our knowledge, the microscopic understanding of this qualitatively different behavior has not been attempted so far, though experimental[10–12] as well as related theoretical work based on model Hamiltonians[13,14] has been performed. One may note that the *B* sublattice, which forms a pyrochlore lattice of corner sharing tetrahedra, is geometrically frustrated in terms of nearest-neighbor (NN) interactions while the *A* sublattice forms a diamond lattice consisting of two interpenetrating face centered cubic (fcc) sublattices which is not frustrated if only NN interactions are assumed. In the following, we will investigate the microscopic origin of the different behavior between FSS and FCS in the framework of density-functional-theory (DFT) calculations. We considered three different basis sets, namely: the linear augmented plane wave (LAPW) method as implemented in the WIEN2K (Ref. 15) code, the muffin-tin orbital (MTO) based *N*th-order MTO (NMTO) method[16] as implemented in the Stuttgart code and the plane-wave basis as implemented in the Vienna *ab initio* simulation package (VASP).[17] The reliability of the calculation in the three basis sets has been cross-checked.

I. CRYSTAL STRUCTURE

Both FCS and FSS crystallize in the cubic $Fd\bar{3}m$ structure. The lattice parameters of FCS and FSS are reported to be 9.99 Å and 10.50 Å,[10,18] respectively, showing a 5% expansion in FSS due to the presence of larger Sc^{3+} ions (size ~0.75 Å) compared to Cr^{3+} ions (size ~0.62 Å). The internal parameter associated with S shows deviations from its ideal value of $\frac{1}{4}$, with 0.259 for FCS and 0.255 for FSS.[18,19] This leads to a trigonal distortion in the BS_6 octahedra measured in terms of the deviation of the S-B-S bond angle from the ideal 90° angle; 4.35° (FCS) and 2.5° (FSS). The tetrahedra remain undistorted in both compounds.

II. ELECTRONIC STRUCTURE

Figure 1 shows nonspin polarized density of states (DOS) calculated in the LAPW basis with the generalized gradient approximation (GGA).[20] In order to check the influence on the electronic properties of the crystal structure differences between FCS and FSS, we have also performed calculations for FSS assuming the crystal structure of FCS. The top panel of Fig. 1 shows the DOS of FSS obtained considering the actual crystal structure in comparison with the DOS obtained assuming the crystal structure of FCS. The bottom panel shows the comparison of DOS between FSS and FCS both in their actual crystal structure. We notice that while the change in crystal structure has some effect (a) in terms of narrowing the Fe *d* dominated states at the Fermi level (E_f) in the actual FSS lattice compared to the results with the hypothetical lattice and (b) in the positioning of the empty Sc levels spanning the energy window of about 1–5 eV (Fig. 1 top panel), the major changes happen upon replacing Sc by Cr (Fig. 1

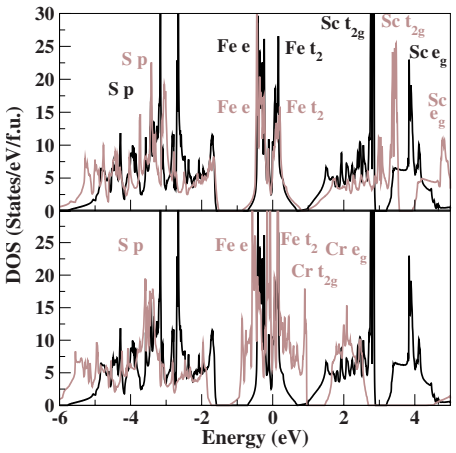

FIG. 1. (Color online) Nonspin-polarized total DOS calculated within GGA with the zero of energy set at E_f. Top panel: DOS of FSS calculated in the actual crystal structure (dark solid line) and in the crystal structure of FCS (light solid line). Bottom panel: comparison DOS of FSS (dark solid line) and FCS (light solid line). The various orbital contributions are marked for each DOS plots.

bottom panel). The bandwidth of the Fe d dominated states crossing E_f is substantially increased and also there is a significant change in the unoccupied region of the spectrum. The difference between the electronic structure of FCS and FSS becomes more evident in the spin polarized band structure shown in Fig. 2. Although FSS does not spin order, such calculations are useful in understanding the relative positions of Fe and the cation B (Cr or Sc) energy levels taking into account the spin degrees of freedom. Fe and Cr/Sc d states are crystal split, in e and t_2, and t_{2g} and e_g, respectively, as well as spin split. In the down spin channel, the Fe d dominated states are completely occupied while in the up-spin channel Fe e states are partially empty in agreement with the Fe^{2+} nominal valence. For Sc, the d states are empty in both spin channels with little shift in the energy scale between the two spin channels, proving the essentially nonmagnetic character of Sc^{3+}. The Cr d states are empty in the down-spin channel and partially occupied in the up-spin channel with t_{2g} up-spin states occupied and e_g up-spin states empty with a spin splitting of about 2 eV. This is in agreement with a ferrimagnetic spin ordering between Fe and Cr. The difference between FCS and FSS arises from the relative energy positions of Cr and Sc with respect to that of Fe. While the Sc d levels all appear above the Fe d states with little mixing between them, there exists a rather strong mixing between Fe d and Cr d states in the up spin channel. It is this Fe-Cr mixing that causes the substantial increase in the width of the Fe d dominated states crossing E_f in Fig. 1. The energy levels of nonspin-split Fe and Cr d states are found to be within an energy window 0.5 eV, causing near degeneracy between the levels, while the Fe and Sc levels are found to be energetically separated by about 2 eV or more.

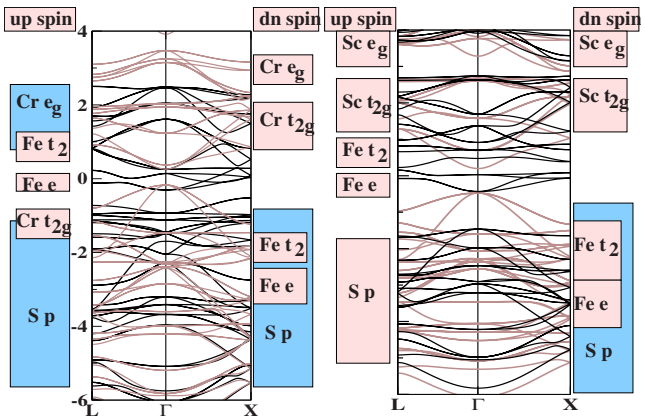

FIG. 2. (Color online) Spin-polarized band structure calculated within GGA. The zero of energy is set at E_f. Left panel shows band structure of FCS and right panel shows the same for FSS. The dark lines (black in color) represent the bands corresponding to up spin channel and light line (gray in color) represent the bands corresponding to down spin channel.

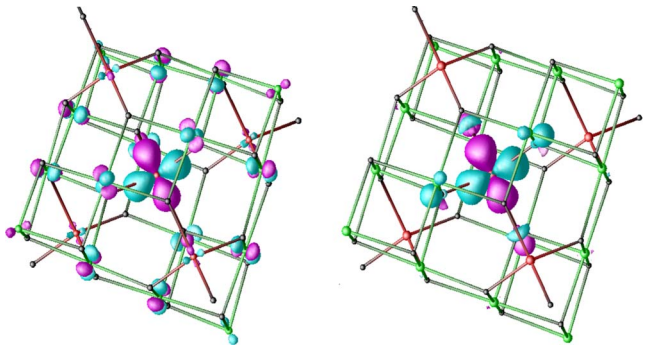

FIG. 3. (Color online) Wannier function plot of Fe d_{xy} orbital for FCS (left panel) and FSS (right panel). Plotted are the constant value surfaces. Two opposite lobes of the wave functions are colored differently.

III. EFFECTIVE FE-FE INTERACTION

In order to extract the effective Fe-Fe interactions we performed NMTO downfolding calculations. Starting from a full DFT calculation, the method constructs the low-energy Hamiltonian defined in an effective Wannier function basis by integrating out degrees of freedom that are not of interest (downfolding). In our downfolding calculations, we have kept active Fe d states and have downfolded all the other states involving Cr/Sc and S. Figure 3 shows the Fe d_{xy} Wannier function for FCS and FSS. The central region of the Wannier function is shaped according to the Fe d_{xy} symmetry while the tails are shaped according to the integrated out orbital degrees of freedom, e.g., Cr/Sc and S orbitals. We first notice that the Wannier function for FCS is much more delocalized compared to that of FSS with significant weights at the Cr sites surrounding the central Fe site. In contrast, the Wannier function for FSS is localized with little weight on Sc sites and only some weight on the neighboring S sites.

The real-space Hamiltonian constructed in the effective Wannier function basis of Fe is tabulated in Table I considering up to second nearest-neighbor (2NN) interactions. Focusing on the hopping parameters listed in Table I and their difference (shown in boldface), we find the changes to be most significant within the $t_2(d_{xy},d_{yz},d_{xz})$ block of the

TABLE I. Hopping matrix elements (in meV) of FSS and FCS (first two values of each column, respectively) and the magnitude of their differences (third value of each column) for the NN ($[\frac{1}{4}\frac{1}{4}\frac{1}{4}]$) and 2NN ($[0\frac{1}{2}\frac{1}{2}]$,$[\frac{1}{2}0\frac{1}{2}]$,$[\frac{1}{2}\frac{1}{2}0]$). The matrix elements are listed for distinct entries only. 1, 2, 3, 4, and 5 represent the five d orbitals, d_{xy}, d_{yz}, d_{3z^2-1}, d_{xz}, and $d_{x^2-y^2}$, respectively.

m,m'	$[\frac{1}{4}\frac{1}{4}\frac{1}{4}]$	$[0\frac{1}{2}\frac{1}{2}]$	$[\frac{1}{2}0\frac{1}{2}]$	$[\frac{1}{2}\frac{1}{2}0]$
1,1	−3 60 **63**	43 12 **31**	43 12 **31**	−16 −13 **3**
2,2	−3 60 **63**	−16 −13 **3**	43 12 **31**	43 12 **31**
3,3	11 10 **1**	−6 −1 **5**	−6 −1 **5**	−21 2 **23**
4,4	−3 60 **63**	43 12 **31**	−16 −13 **3**	43 12 **31**
5,5	11 10 **1**	−16 1 **17**	−16 1 **17**	−1 −2 **1**
1,2	−10 −9 **1**	−22 11 **33**	46 17 **29**	22 −11 **33**
1,3	−22 −18 **4**	16 8 **8**	16 8 **8**	−11 −22 **11**
1,4	−10 −9 **1**	46 17 **29**	−22 11 **33**	22 −11 **33**
1,5	0 0 **0**	−18 3 **21**	18 −3 **21**	0 0 **0**
2,3	11 9 **2**	4 11 **7**	7 −7 **0**	−24 −1 **23**
2,4	−10 −9 **1**	22 −11 **33**	−22 11 **33**	46 17 **29**
2,5	−19 −16 **3**	−7 −19 **12**	23 5 **18**	5 8 **3**
3,4	11 9 **2**	−7 7 **14**	4 11 **7**	24 1 **23**
3,5	0 0 **0**	9 −2 **11**	−9 2 **11**	0 0 **0**
4,5	19 16 **3**	−23 −5 **18**	7 19 **12**	−5 −8 **3**

Hamiltonian. We observe that while for FCS, the Fe-Fe NN hopping integrals are larger than the 2NN hopping terms (the largest 2NN is about three times smaller than the largest NN hopping term), the reverse is the case for FSS where the 2NN hoppings are larger than the NN hoppings (the largest 2NN hopping is twice as big as the NN hopping). The NN and 2NN paths between two A ions in a spinel lattice, as shown in Fig. 4, are A-X-B-X-A exchange paths. The NN interaction connects A ions of two FCC sublattices while the 2NN interaction connects A ions within the same FCC sublattice. The large value of the 2NN interaction can therefore generate strong frustration.

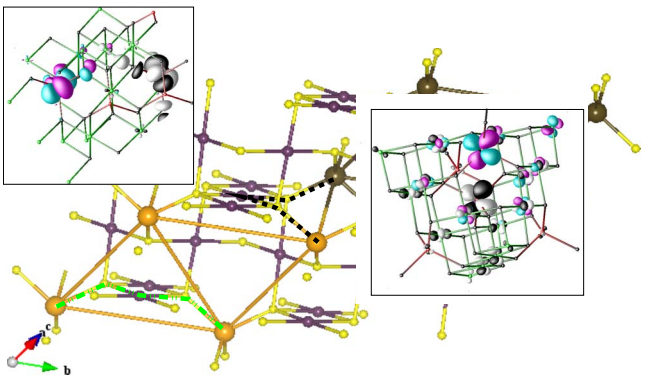

FIG. 4. (Color online) The NN and 2NN interaction path between Fe atoms. Small dark and light balls represent B(Sc/Cr) and S atoms, respectively. Big dark and light balls represent Fe atoms belonging to two FCC sublattices constituting the diamond lattice. The dashed line in black (dark) and green (light), represent the NN and 2NN paths, respectively. The inset in the upper-left (lower-right) corner shows the overlap of the Wannier functions of Fe d_{xy} placed at two Fe atoms in FSS (FCS) separated by 2NN (NN) distance.

The NN hopping path as marked in Fig. 4, includes Fe-B-Fe, Fe-S-Fe, and S-B-S bond angles of about 60°, 80°, and 90°, respectively, while the corresponding bond angles for the 2NN hopping paths are found to be close to 120°, 130°, and 90°, respectively.[21] For the NN it is therefore the direct Fe-B hybridization that becomes important, with anions playing little role while for the 2NN interaction, the anion mediated (Fe-S-Fe) exchange becomes important. The fact that the NN interaction is strong in FCS and the 2NN interaction is strong in FSS is supported by the plot of the Wannier functions for two NN Fe sites (top left panel of Fig. 4) and two 2NN Fe sites (bottom right panel of Fig. 4). For FCS, we find a clear overlap of Cr-like tails between two Wannier functions while for FSS the S-like tails point to each other.

The exchange interaction may be derived from the hopping integrals through the use of a superexchangelike formula. This however needs the knowledge of the appropriate charge-transfer energy, which is difficult to estimate because of complicated hopping paths. We therefore preferred to compute the effective magnetic exchange interactions between Fe ions in terms of total energy calculations of different spin arrangements of Fe and mapping the total energies to an Ising-type model defined in terms of Fe spins. For this purpose, spin-polarized calculations were carried out with a plane wave basis as implemented in VASP and with the choice of the GGA exchange-correlation functional. While admittedly such calculations are faced with several difficulties such as the choice of spin configurations in supercells, particularly since it involves small energies, it is expected to provide us with relative strength of various exchange interactions as well as some order of magnitude estimates. For FSS, our calculations gave $J_1=-0.01$ meV (NN) and $J_2=-0.37$ meV (2NN) with $J_2/J_1=37$; the 2NN interaction dominates the NN interaction, as already inferred from the hopping parameters. This is in agreement with the findings of neutron scattering measurements.[11] For FCS we obtained $J_1=6$ meV and $J_2=2.5$ meV both being of ferromagnetic nature, in agreement with the observed ferromagnetic spin ordering within the Fe sublattice. The NN interaction dominates over the 2NN neighbor interaction in this case with $J_2/J_1=0.4$ in sharp contrast with that of FSS.

IV. SPIN-ORBIT COUPLING

Due to the presence of unquenched orbital degrees of freedom on the Fe sites, the importance of the spin-orbit (SO) coupling in these compounds has been discussed[13] in the past. An important quantity in this context is the relative strength of the SO coupling parameter, λ, with respect to the dominant spin exchange. In Table II we show the magnetic moments at the Fe and B(Cr/Sc) site obtained from a GGA+U+SO calculation in LAPW basis carried out for FCS and FSS by considering a $J=1$ eV (Hund's coupling) and $U=2.5$ eV at the Fe site due to the Coulomb renormalization of the spin-orbit splitting, as found previously.[22] A

TABLE II. Magnetic moments of Fe and B(Cr/Sc) ions in μ_B and anisotropy energy in meV/Fe.

	Fe		B(Cr/Sc)		Anisotropy energy (meV/Fe)
	Orbital moment	Spin moment	Orbital moment	Spin moment	
FCS	−0.13	−3.27	−0.03	2.69	10
FSS	−0.14	−3.44	0.0	0.05	6

rather large moment of 0.13–0.14 μ_B pointing along the same direction as the spin moment has been obtained at the Fe site for both FCS and FSS. Such values are surprisingly large given the fact that the orbitally active levels of Fe are e levels. This has been rationalized in terms of finite coupling between Fe e and empty t_2 orbitals.[22] Table II also lists the magnetocrystalline anisotropy energy obtained as the total energy difference between the calculations with the spin quantization along [001] and [110]. The anisotropy energy is found to be almost two times larger for FCS compared to FSS, indicating stronger spin-orbit interaction in FCS. The strength of the effective spin-orbit interaction depends on the energy level separation (Δ) between Fe e and t_2. We have estimated Δ from the NMTO-downfolding calculations in the effective Fe only basis, and obtain[23] $\Delta=0.46$ eV for FSS and $\Delta=0.20$ eV for FCS. Using second-order perturbation theory[24] as considered in Ref. 13, the spin-orbit coupling parameter is given by $\lambda \sim \frac{6\lambda_0^2}{\Delta}$, where λ_0 is the atomic spin-orbit coupling constant, estimated to be 0.01 eV.[25] We obtain $\lambda=1.3$ meV (FSS) and 3 meV (FCS). Considering the dominant magnetic interaction into account, $\frac{J}{\lambda}$ is $\gg 1$ in FCS and $\ll 1$ in FSS. As discussed in Refs. 13, these two situations will give rise to very different ground states, an magnetically ordered state for $\frac{J}{\lambda} \gg 1$ and a spin orbital singlet for $\frac{J}{\lambda} \ll 1$.

To conclude, we have carried out DFT calculations to provide a microscopic understanding of the dissimilar behavior of spinel compounds FCS and FSS, both having orbitally active A ions. We found that this originates from the difference in the hybridization between Fe d states and B (B=Cr/Sc) states and S p states. This not only affects the magnitude of magnetic exchanges but also the relative importance of different magnetic exchanges: a contrasting value of J_2/J_1 of 37 in the case of the Sc compound to a value of 0.4 in the case of the Cr compound. Moreover, the J's are antiferromagnetic for the Sc systems and ferromagnetic for the Cr system. This leads to important frustration effects in the Sc compound which are absent in the Cr compound. In our entire analysis, we have not considered the effect of Jahn-Teller (JT) interactions. Though crystallographically no signature for static JT order has been found, there could be dynamic JT effects. This will be taken up in a future study.

ACKNOWLEDGMENTS

T.S.D. would like to acknowledge support from DST through AMRU project. S.S. thanks CSIR for financial support. R.V. thanks the DFG for financial support through the SFB/TRR 49 program. Authors would like to thank J. Deisenhofer for discussion.

[1] P. G. Radaelli, New J. Phys. **7**, 53 (2005).
[2] O. Tchernyshyov, Phys. Rev. Lett. **93**, 157206 (2004).
[3] S. Di Matteo, G. Jackeli, and N. B. Perkins, Phys. Rev. B **72**, 020408 (2005).
[4] T. Maitra and R. Valentí, Phys. Rev. Lett. **99**, 126401 (2007).
[5] V. O. Garlea, R. Jin, D. Mandrus, B. Roessli, Q. Huang, M. Miller, A. J. Schultz, and S. E. Nagler, Phys. Rev. Lett. **100**, 066404 (2008).
[6] S. Sarkar, T. Maitra, Roser Valentí, and T. Saha-Dasgupta, Phys. Rev. Lett. **102**, 216405 (2009).
[7] G.-W. Chern, N. Perkins, and Z. Hao, Phys. Rev. B **81**, 125127 (2010).
[8] P. G. Radaelli, Y. Horibe, M. J. Gutmann, H. Ishibashi, C. H. Chen, R. M. Ibberson, Y. Koyama, Y.-S. Hor, V. Kiryukhin, and S. Cheong, Nature (London) **416**, 155 (2002).
[9] M. Schmidt, W. Ratcliff, P. G. Radaelli, K. Refson, N. M. Harrison, and S. W. Cheong, Phys. Rev. Lett. **92**, 056402 (2004).
[10] M. S. Park, S. K. Kwon, S. J. Youn, and B. I. Min, Phys. Rev. B **59**, 10018 (1999).
[11] A. Krimmel, M. Mücksch, V. Tsurkan, M. M. Koza, H. Mutka, and A. Loidl, Phys. Rev. Lett. **94**, 237402 (2005).
[12] N. Büttgen, J. Hemberger, V. Fritsch, A. Krimmel, M. Mücksch, H.-A. Krug von Noida, P. Lunkenheimer, R. Ficht, V. Tsurkan, and A. Loidl, New J. Phys. **6**, 191 (2004).
[13] G. Chen, A. P. Schnyder, and L. Balents, Phys. Rev. B **80**, 224409 (2009); G. Chen, L. Balents, and A. P. Schnyder, Phys. Rev. Lett. **102**, 096406 (2009).
[14] D. Bergman, J. Alicea, E. Gull, S. Trebst, and L. Balents, Nat. Phys. **3**, 487 (2007).
[15] P. Blaha, K. Schwartz, G. K. H. Madsen, D. Kvasnicka, and J. Luitz, *wien2k, An Augmented Plane Wave Plus Local Orbitals Program for Calculating Crystal Properties*, edited by K. Schwarz (Technische Universität Wien, Austria, 2001).
[16] O. K. Andersen and T. Saha-Dasgupta, Phys. Rev. B **62**, R16219 (2000).
[17] G. Kresse and J. Hafner, Phys. Rev. B **47**, 558 (1993); **49**, 14251 (1994).
[18] A. Krimmel (private communication).
[19] G. Shirane and D. E. Cox, J. Appl. Phys. **35**, 954 (1964).
[20] J. P. Perdew, K. Burke, and M. Ernzerhof, Phys. Rev. Lett. **77**, 3865 (1996).
[21] The numbers differ only slightly between FCS and FSS.
[22] S. Sarkar, Molly De Raychaudhury, I. Dasgupta, and T. Saha-Dasgupta, Phys. Rev. B **80**, 201101(R) (2009).
[23] Δ is found to be smaller for FCS compared to FSS due to significant mixing of Fe and Cr d states in FCS and absence of such effects in FSS.
[24] J. T. Vallin, Phys. Rev. B **2**, 2390 (1970).
[25] C. Testelin, C. Rigaux, A. Mauger, A. Mycielski, and C. Julien, Phys. Rev. B **46**, 2183 (1992).